Journal of Geographical Research & Report
Volume 1, Issue 1 | December 2025 | DOI: 10.64712/jgeorr.v1i1.652

Hydrogeochemical characterization and evolution of groundwater in parts of the Western and Central Regions of Ghana

Millicent Obeng Addai[1]

[1]Department of Geography Education, University of Education, Winneba, Ghana

Email: moaddai@uew.edu.gh

Abstract

Groundwater serves as a critical resource for domestic, agricultural, and industrial use across southern Ghana, particularly in rural and peri-urban areas. This study evaluates the hydrogeochemical characteristics and suitability of groundwater in parts of the Western and Central Regions, covering Wassa Amenfi East, Tarkwa-Nsuaem, Twifo Atti Morkwa, and Assin North districts. Forty-eight groundwater samples were collected during the transition between the rainy and dry seasons in August and analysed for major ions, heavy metals, and key physicochemical parameters. Results showed that while most samples were within WHO limits for parameters such as NO_3^-, HCO_3^-, and PO_4^{3-}, elevated concentrations of EC, TDS, Na^+, Cl^-, SO_4^{2-}, F^-, and Mn were observed in mining-influenced areas, indicating salinization and contamination risks. Multivariate analysis (PCA and HCA) identified key hydrogeochemical processes including silicate and carbonate weathering, sulfide oxidation, redox transitions, and anthropogenic pollution from agriculture and sanitation. Groundwater facies were predominantly Ca–Mg–Cl–SO_4, consistent with mineralized bedrock influence, while samples in recharge zones showed Ca–Mg–HCO_3 characteristics. Irrigation indices yielded mixed results: although 58% of samples were classified as "Good" to "Permissible" based on Na%, SAR, and PI, all samples exceeded the RSBC threshold, suggesting potential hazards to soil permeability due to excess bicarbonate. Pollution indices revealed localized zones of moderate nitrate contamination and elevated fluoride levels, with 25% of samples exceeding PIG thresholds, especially in areas with intensive land use. These findings underscore the spatial variability and vulnerability of groundwater quality in the region, driven by both geological and anthropogenic factors.

Keywords: Groundwater quality, Hydrogeochemistry, Pollution indices, Irrigation suitability, Birimian Supergroup, Southern Ghana

To cite this article: Addai (2025). Hydrogeochemical characterization and evolution of groundwater in parts of the Western and Central Regions of Ghana. *Journal of Geographical Research & Report*, 1 (1). 10.64712/jgeorr.v1i1.652

1 Introduction

Groundwater remains a vital resource across Ghana, serving as a dependable supply for drinking, irrigation, and other domestic and industrial needs, particularly in rural and peri-urban areas (Akurugu et al., 2020; Abanyie et al., 2018). National estimates suggest that over 70% of the population depend on groundwater for their daily water needs (Akurugu et al., 2020). However, increasing anthropogenic pressure, primarily through mining and agriculture, poses significant threats to the chemical and physical integrity of these aquifers. In the forested transition belt between Ghana's Western and Central Regions, these concerns are particularly acute, given the dual intensification of mining and agro-based land use (Owusu-Nimo et al., 2018; Amuah et al., 2022).

This geological zone is historically significant for its gold endowment and mineralization, with an extensive network of both large-scale and artisanal gold mining operations. Simultaneously, these districts support intensive farming systems, especially cocoa cultivation and food crop production, often accompanied by chemical inputs such as fertilizers and pesticides. Together, these activities generate non-point and point source contaminants, increasing the likelihood of groundwater degradation (Douti et al., 2021; Bekoe et al., 2021).

The area's hydrogeological system is shaped not only by anthropogenic inputs but also by natural factors such as aquifer lithology, groundwater–rock interaction, and weathering processes (Kazapoe et al., 2024). The dominance of Birimian metasediments, granitoids, and associated weathering profiles is expected to influence the distribution of major ions and trace metals in groundwater, especially in areas underlain by amphibolites and granitic intrusions (Buamah et al., 2008; Hadzi et al., 2018). Moreover, river systems such as the Pra and Ankobra basins serve as key surface–groundwater interfaces, enhancing recharge but also presenting vulnerability to contamination (Ganyaglo et al., 2012). Although previous studies have characterized groundwater quality in isolated parts of the Western and Central Regions (Akoto et al., 2019; Obiri, 2007), a region-wide, systematic hydrogeochemical assessment incorporating both domestic and irrigation suitability remains limited. This study addresses that gap by conducting a comprehensive hydrogeological and geochemical assessment of groundwater across the four districts. The analysis covers both natural and anthropogenic influences on water quality and investigates key parameters such as pH, electrical conductivity, major cations and anions, and heavy metals.

Similar hydrogeochemical challenges are reported in other tropical mineralized terrains worldwide. For example, studies in the Brazilian Amazon have documented elevated iron, manganese, and mercury in groundwater linked to gold mining and lateritic weathering (Malm et al., 1995). In India's Precambrian shields, groundwater is often enriched in fluoride, nitrate, and salinity due to the combined effects of hard-rock aquifers and intensive agriculture (Subba Rao & Rao 2010). Southeast Asian terrains such as northern Thailand and Laos also exhibit groundwater contamination from sulfide oxidation in mining belts, with elevated sulfate and heavy metals (Williams et al., 1996). These parallels demonstrate that mineralized tropical terrains are globally vulnerable to coupled geogenic and anthropogenic influences on groundwater quality. By situating the Ghanaian case within this wider context, the study underscores the relevance of its findings to other regions with similar geological and land-use settings.

Guided by these concerns, the study seeks to uncover the dominant hydrogeochemical processes that shape groundwater quality in the transition zone between the Western and Central Regions of Ghana. It further examines the suitability of groundwater for both domestic and irrigation purposes and identifies potential contamination of hotspots arising from mining and agricultural pressures. In doing so, the study proceeds from three working hypotheses: first, that groundwater quality is jointly controlled by geogenic factors such as silicate and carbonate weathering and sulfide oxidation, together with anthropogenic influences from mining and agriculture; second, that a substantial proportion of groundwater sources exceed WHO thresholds for key parameters including sodium, chloride, sulfate, manganese, and fluoride, particularly in mining-impacted zones; and third, that irrigation suitability is limited by sodicity and residual sodium bicarbonate levels, which threaten long-term soil productivity in this agrarian region.

The overarching aim is to evaluate the spatial variability and quality of groundwater for multiple uses, with particular attention to the influence of underlying geology, land use, and proximity to pollution sources. This research not only contributes to the broader understanding of groundwater systems in tropical mineralized terrains but also provides practical insights for sustainable groundwater management. Ultimately, the findings are intended to inform water resource policy, improve public health safeguards, and enhance land-use planning in one of Ghana's most ecologically and economically critical zones.

2 Methodology

2.1 Study area

The study area falls within the transition zone between the Western and Central Regions of Ghana, specifically covering parts of the Wassa Amenfi East, Tarkwa-Nsuaem, Twifo Atti Morkwa, and Assin North Districts, as shown in Figure 1. The region is located within the southern portion of Ghana and is geologically and hydrogeologically significant due to its position along the Birimian Supergroup terrain, which hosts numerous mineralized zones (Junner, 1940; Hirdes, et al., 1992). The Wassa Amenfi East District, located on the western edge of the map, borders Tarkwa-Nsuaem to the south and Twifo Atti Morkwa to the east. The Assin North Municipal, situated toward the northeastern corner of the map, lies within the Central Region and is bounded by Twifo Atti Morkwa and Asikuma-Odoben-Brakwa to the south. The area is drained by several river systems, including tributaries of the Pra and Ankobra Rivers, which form important drainage basins for both domestic and agricultural water supply (Ganyaglo et al., 2012). Accessibility within the area is facilitated by a network of regional and feeder roads, notably the Kumasi–Takoradi and Cape Coast–Assin Foso–Twifo Praso roads, which link major settlements such as Assin Foso, Twifo Praso, and Tarkwa. While major highways are generally motorable year-round, several smaller feeder roads experience reduced accessibility during the rainy season, particularly in heavily forested and undulating areas (Gibrilla et al., 2010; Kazapoe et al., 2023).

The study area lies within Ghana's semi-equatorial climatic zone (Dickson & Benneh, 1988). This region typically experiences a bimodal rainfall pattern, with total annual precipitation ranging from 1,200 mm to 2,000 mm. The major rainy seasons occur between May and June, and again from September to October. Dry conditions are most noticeable between February and April. Average annual temperatures range from 24°C to 29°C, with the hottest period (around 30°C) typically occurring in March and April, and the coolest (approximately 26°C) in August. Relative humidity peaks during the rainy seasons, averaging between 75% and 80%, and drops during the drier months. The terrain is predominantly undulating to hilly, with localized valleys occupied by seasonal and perennial streams. The topography gradually rises westward into the forest-dominated Wassa landscape, with elevations generally increasing toward the boundary with the Ashanti Region. This physiographic setting influences the distribution of land use, hydrology, and groundwater potential, with weathered zone aquifers primarily developed along hill slopes and fracture-controlled systems present in the granitoid units (Gibrilla et al., 2010; National Research Council, 1996). Given the region's complex lithological structure, access to clean and sustainable groundwater is often influenced by geological contacts,

including zones of shearing, intrusions, and fractured granite-gneiss formations (Ganyaglo et al., 2010; Gibrilla et al., 2011). These natural conditions, combined with population growth and mineral development, make the area a focal point for hydrogeological and environmental assessments.

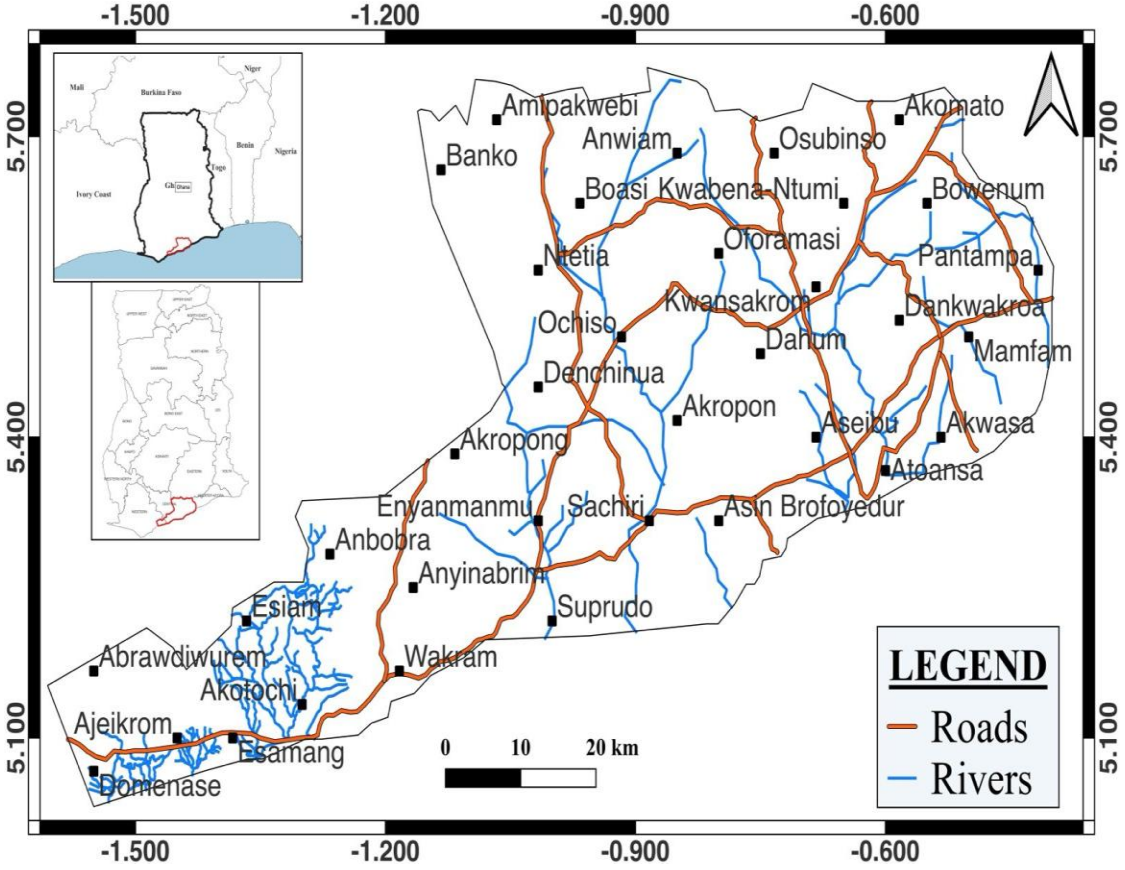

Figure 1: Map of the study area

2.2 Sampling Design

Forty-eight (48) groundwater samples were collected from hand-dug wells and boreholes across the study area. The samples were collected during the transition between the rainy and dry seasons in August. Each sampling site was annotated on the field map for spatial referencing and cross-validation with geochemical datasets. At each location, three replicate samples were collected to improve analytical reliability and account for temporal variation. A purposive stratified sampling approach was employed to ensure that the selected groundwater sources adequately represented the hydrogeological and land-use diversity of the study area. The strata included mining-impacted zones, agricultural areas, and relatively undisturbed settings. Within each stratum, boreholes and hand-dug wells were purposively chosen based on accessibility, functionality, and local usage for drinking and irrigation. This strategy enabled the study to capture both geogenic and anthropogenic influences on groundwater quality. At each site, three replicate

samples were collected to account for temporal variation and improve analytical reliability. Two 0.5 L opaque plastic bottles were used at every site: one for cation and heavy metal analysis and the other for anions. Bottles were prewashed with a 1:1 solution of concentrated nitric acid (HNO_3) and distilled water and then rinsed thoroughly with distilled water to prevent contamination (American Public Health Association APHA, 2017). Before sampling, each bottle was rinsed three times with the sample water. For heavy metals, one of the bottles was acidified to pH < 2 with concentrated HNO_3 to prevent adsorption and precipitation of trace elements (Sulaiman et al., 2024). For anion analysis, water was drawn with a 50 mL syringe, passed through a 0.45 µm membrane filter, and transferred into a separate labelled bottle. All samples were stored at <5 °C in an ice chest in the field and later refrigerated at 4 °C at the Ghana Atomic Energy Commission (GAEC) laboratory prior to analysis. This procedure ensured the preservation of redox-sensitive species and compliance with quality assurance protocols (APHA, 2017).

Field parameters were measured immediately upon sample collection to reflect native groundwater conditions. These included temperature, pH, electrical conductivity (EC), total dissolved solids (TDS), salinity, alkalinity, and geographical coordinates. A TeraCon 325 multiparameter meter was used for EC, TDS, salinity, and temperature, while a calibrated pH meter was used for pH measurements. Alkalinity and total hardness were determined via titrimetric methods using standard procedures (Harris, 2007; APHA, 2017). Table 1 lists all parameters and their respective measurement techniques. The Cation concentrations, including Na^+ and K^+ were determined using a flame photometer, while Ca^{2+} and Mg^{2+} were quantified using EDTA titration. Anions such as Cl^-, SO_4^{2-}, and NO_3^- were analysed with a Dionex ICS-90 ion chromatograph. Heavy metals, including As, Pb, Zn, Cu, and Fe, were determined using Atomic Absorption Spectrophotometry (AAS), consistent with international best practices for trace element analysis in groundwater (Olayinka et al., 2017). The selection of these metals was informed by their association with hydrothermal alteration and ore fluid pathways common to orogenic gold systems in West Africa.

Strict QA/QC protocols were followed throughout the sampling and analysis phases. Plastic bottles were sterilised and preserved in autoclaved bags before field deployment. Sterile gloves were worn and changed between sampling locations to avoid cross-contamination. Field blanks were collected under the same conditions as regular samples and sent for analysis to monitor background contamination (Sulaiman et al., 2024). Samples were analyzed in triplicate where feasible, and intra-laboratory consistency was ensured by using a single laboratory (GAEC) and a designated analyst to minimise analytical variability. Containers were rinsed with

site-specific water before final sampling, simulating local water retrieval practices (e.g., via rope and bucket), to maintain realism in the hydrochemical profile. All instruments were calibrated daily, and reagents were prepared with analytical-grade chemicals to ensure accuracy and reliability of results (APHA, 2017).

To enhance analytical transparency, the detection limits for each parameter were documented (Table S1). AAS detection limits were 0.001 mg/L for As, 0.005 mg/L for Pb, 0.01 mg/L for Cu, 0.002 mg/L for Zn, and 0.005 mg/L for Mn. For anions measured by ion chromatography, the detection limits were 0.02 mg/L for Cl^-, 0.05 mg/L for SO_4^{2-}, and 0.1 mg/L for NO_3^-. Flame photometry detection limits were 0.1 mg/L for Na^+ and K^+, while EDTA titration methods had quantification thresholds of 1.0 mg/L for Ca^{2+} and Mg^{2+}. These values align with APHA (2017) standards and GAEC laboratory protocols. Analytical uncertainties were assessed through triplicate analysis of selected samples, with relative standard deviations (RSDs) below 5% for major ions and below 10% for trace metals. Daily calibration of AAS and ion chromatograph instruments using certified standards further minimized systematic errors. Field duplicates and blanks were also analysed, showing negligible contamination. Although minor variability was observed between replicates, the differences were within acceptable analytical error margins and did not affect water quality classification outcomes.

2.3 Suitability of groundwater for Irrigation purposes

Residual Sodium Bicarbonates (RSBC) and Percentage Sodium (Na%) of the samples were determined following Gupta and Gupta (1987) and Wilcox (1955) as indicated in Equations 1 and 2, respectively.

$$\text{RSBC} = [HCO_{3-} - Ca^{2+}] \quad (1)$$

$$\text{Na\%} = \left[\left[\frac{Na^{2+}}{(Na^{2+} + K^{+} + Ca^{2+} + Mg^{2+})}\right] x\ 100\right] \quad (2)$$

Table 1: RSBC (WHO, 1989) and Na% (Wilcox, 1955) classifications

RSBC		Na%	
Range	Irrigation class	Quality of water	Na% value
< 1.25	Safe for irrigation	Excellent	< 20
1.25 – 2.50	Marginal	Good	20 – 40
> 2.50	Unsuitable for irrigation	Permissible	40 – 60
		Doubtful	60 – 80
		Unsuitable	> 80

Following Richards (1954) and Doneen (1964), the Sodium Absorption Ratio (SAR) and Permeability Index (PI) were computed as presented in Eqn. 3 and 4.

$$\text{SAR} = \frac{Na^{+}}{\sqrt{\frac{Ca^{2+} + Mg^{2+}}{2}}} \quad (3)$$

$$PI = \left[\left[\frac{(Na^{2+} + \sqrt{HCO_3})}{(Na^{2+} + K^{+} + Ca^{2+} + Mg^{2+})}\right] x\ 100\right] \quad (4)$$

Table 2: SAR (Richards, 1954) and PI (Sappa et al., 2014) descriptions

SAR			PI	
Value	Water quality	Range (%)	Class	Classification
< 10	Excellent water	< 25	I	Unsuitable water for irrigation
10 – 18	Good water	25 – 75	II	Suitable water for irrigation
18 – 26	Doubtful	> 75	III	Suitable water for irrigation
> 26	Unsuitable water			

Magnesium Hazards (MH) was also measured following the formulas, respectively, presented by Szabolcs and Darab (1964) presented as:

$$MH = \left[\frac{(100\ X\ Mg^{2+})}{(Ca^{2+} + Mg^{2+})}\right] \quad (5)$$

Table 3: Magnesium Hazards (MH) (Prasanth et al., 2012)

MH % value	Quality of water
< 50	Suitable for irrigation
50	Unsuitable for irrigation

2.4 Pollution Index of Groundwater (PIG)

The Pollution Index of Groundwater (PIG) provides a comprehensive measure of groundwater pollution by integrating multiple water quality parameters. It is calculated using equations 6-9:

$$WP = \frac{RW}{\sum RW} \quad (6)$$

$$SOC = \frac{C_i^n}{DWQS} \quad (7)$$

$$OQG = WP \times SOC \quad (8)$$

$$PIG = \sum OQG \quad (9)$$

Where C_i^n is the observed concentration, DWQS is the drinking water quality standard, WP is the weighting coefficient, RW is the relative weight, and OQG is the overall quality groundwater.

2.5 Fluoride Pollution Index (FPI)

Fluoride contamination in groundwater is assessed using the Fluoride Pollution Index (FPI). FPI is calculated using equation (5):

$$FPI = \frac{W_f + W_{HCO3} + W_{Na/Ca} + W_{pH}}{N(parameters)} \quad (10)$$

Where N is the total amount of groundwater elements, W_{pH} represents the pH weight; $W_{Na/Ca}$ is the Na+/Ca+ ratio weight, W_{HCO3} is the bicarbonate weight, and W_f is the fluoride weight.

2.6 Nitrate Pollution Index (NPI)

The Nitrate Pollution Index (NPI) evaluates groundwater nitrate contamination and is computed using equation (11):

$$NPI = \frac{C_s - HAV}{HAV} \quad (11)$$

Where C_s is the measured nitrate concentration, and HAV is the permissible nitrate value.

2.7 Factor Analysis / Principal Component Analysis

The same set of parameters used for the correlation matrix was analyzed via Principal Component Analysis (PCA) or Exploratory Factor Analysis. Before running the analysis, data were mean-centred and scaled to unit variance if parameters were measured in different units or on different scales. Prior to PCA, all variables were standardized to z-scores to ensure comparability across different units of measurement. Data normality was evaluated using Shapiro–Wilk tests and descriptive statistics of skewness and kurtosis. While some variables showed moderate departures from normality, PCA is known to be robust under such conditions, given an adequate sample size (n = 48). Linearity among variables was confirmed through correlation analysis, with significant associations observed

among major ions and salinity indicators. Sampling adequacy for PCA was further assessed using the Kaiser–Meyer–Olkin (KMO) test, which exceeded the threshold value of 0.6, and Bartlett's test of sphericity, which was statistically significant ($p < 0.001$). Together, these diagnostics indicate that the dataset met the assumptions required for meaningful factor extraction. The number of factors or principal components retained was determined using eigenvalues >1. Factor loadings or component loadings were examined to interpret which variables contributed most strongly to each factor. For accurate visualization of the results from the PCA, a two-dimensional biplot was generated, using the first two factors or principal components. Sample points were plotted according to their factor/component scores, while variables (arrows) indicate loadings. Sample points were colour-coded based on which factor or cluster they predominantly load on. The factor analysis, as well as its associated biplot, was conducted using the Python language.

2.8 Hierarchical Cluster Analysis

The normalized data matrix (rows = samples, columns = parameters) was used for hierarchical clustering. The Euclidean distance metric and Ward's linkage method were applied to construct a dendrogram, which visually grouped hydrochemical parameters based on their similarity. Samples (rows) and parameters (columns) were clustered independently. In addition, a heatmap was generated where colour intensity represents the magnitude of each parameter in each sample, allowing patterns of similarity and divergence to be easily observed. Together, the dendrogram and heatmap provided complementary views of the clustering structure. All computations and visualizations were performed in Python using the SciPy and Seaborn libraries.

3 Results

3.1 Distribution of physicochemical and hydrochemical parameters in groundwater samples

The summary of the statistics of the physicochemical parameters measured in the groundwater samples is presented in Table 4. It is acknowledged that measurement uncertainty is inherent in hydrochemical analysis. However, the low RSD values, strict QA/QC protocols, and cross-validation with certified standards provide confidence that analytical uncertainties did not materially affect the interpretation of groundwater quality or suitability indices. pH values ranged from 5.76 to 8.88 (mean = 7.14), generally within the WHO (2017) permissible range of 6.5–8.5. However, 16.33% of samples were acidic (pH < 6.5), suggesting interaction with sulfide-bearing lithologies or anthropogenic acidification, particularly near artisanal mining zones (Appelo & Postma, 2005). Acidic groundwater may be corrosive and lead to metal

leaching or skin and eye irritation (WHO, 2011). Turbidity and colour recorded maximum values of 1715 NTU and 875 Hazen units, respectively, with extreme positive skewness (>6) and high kurtosis (>40), indicating highly turbid outliers. While not directly regulated as chemical contaminants, elevated levels suggest poor aesthetic quality and possible microbial risk, especially in wells lacking sanitary protection (WHO, 2017). EC ranged from 96.5 to 48,900 µS/cm (mean = 2,570 µS/cm), far exceeding the WHO limit of 1,500 µS/cm in numerous samples. Similarly, TDS values (53.1–26,895 mg/L; mean = 1,46A4.7 mg/L) show wide variability, with a distribution heavily skewed toward higher concentrations. These trends suggest intense water–rock interaction, particularly in fractured and mineralized zones of the Birimian Supergroup, as well as possible anthropogenic enrichment through mining and agrochemical use (Ganyaglo et al., 2012). Na^+ concentrations were highly variable (6.5–13,980 mg/L; mean = 478.1 mg/L), with many samples exceeding the WHO threshold of 200 mg/L. Elevated Na^+ may be attributed to ion exchange in clay-rich lithologies, fertilizer residues, or waste effluents. Chronic intake of high Na^+ levels may lead to hypertension and kidney dysfunction (Lanjwani et al., 2019). K^+ ranged from 2 to 200 mg/L (mean = 14.9 mg/L), slightly above the WHO desirable limit of 12 mg/L. Its high variability and skewness suggest localized fertilizer input or weathering of K-bearing silicates. Ca^{2+} and Mg^{2+} values were also elevated, with Ca^{2+} ranging from 4 to 1,540 mg/L (mean = 88.5 mg/L) and Mg^{2+} from 0.5 to 1,895 mg/L (mean = 75.2 mg/L). These exceed the WHO desirable limits of 75 mg/L (Ca^{2+}) and 50 mg/L (Mg^{2+}), and may contribute to elevated TH. Their distributions indicate the influence of carbonate and mafic lithologies, especially near mineralized belts.

Inferred from Ca^{2+} and Mg^{2+} levels, TH ranged from 3 to 195.9 mg/L. Approximately 21% of samples exceeded the WHO desirable limit of 100 mg/L. Though not a health concern, elevated TH may impact household plumbing and soap efficiency (WHO, 2011). Cl^- concentrations were highly skewed (mean = 790.7 mg/L; max = 20,249 mg/L), exceeding the WHO limit of 250 mg/L in many cases. The likely sources include household wastewater, agricultural inputs, and evaporite dissolution (Appelo & Postma, 2005). SO_4^{2-} levels (3.21–2,235 mg/L; mean = 135.4 mg/L) were mostly within the WHO limit of 250 mg/L, though some outliers likely reflect the oxidation of sulfide minerals, common in Birimian gold belts. PO_4^{3-} (mean = 0.32 mg/L) was within safe limits. High skewness suggests localized anthropogenic influence, possibly from fertilizers or septic seepage. NO_3^- ranged from 0.01 to 31.4 mg/L (mean = 9.01 mg/L), remaining below the WHO guideline of 50 mg/L. These levels, while modest, may reflect moderate agricultural influence with plant uptake and denitrification buffering concentrations (WHO, 2011; Dorleku et al., 2019). NO_2^- levels, though low in absolute terms (mean = 0.31 mg/L), showed high skewness (6.89), indicating potential for recent pollution from organic decomposition or

malfunctioning sanitation systems. F^- concentrations ranged from 0.01 to 3.27 mg/L (mean = 0.58 mg/L). Some samples exceeded the WHO maximum of 1.5 mg/L, although the general range is consistent with areas underlain by F^--poor lithologies. Prolonged exposure to elevated F^- may pose risks of dental or skeletal fluorosis (WHO, 2017; Ruiz-Pico et al., 2019). HCO_3^- concentrations (17.1–525 mg/L; mean = 133.7 mg/L) reflect the dissolution of carbonates and silicate weathering, as well as CO_2 absorption from recharging waters. These values suggest effective buffering capacity with no known health risk (Appelo & Postma, 2005). NH_3 levels were generally low (mean = 0.13 mg/L), though the upper range (0.82 mg/L) indicates possible organic pollution. Mn, a naturally occurring metal, peaked at 0.86 mg/L (mean = 0.12 mg/L), exceeding the WHO aesthetic limit of 0.4 mg/L in some samples. Elevated Mn can affect taste and stain laundry or plumbing fixtures. TSS values (1–190 mg/L; mean = 17.44 mg/L) support observed turbidity trends, especially in wells with shallow construction or poor casing.

Construction or poor casing.

Table 4: Summary statistics of physicochemical parameters evaluated in this study

	Min	Max	Mean	Skewness	Kurtosis
pH	5.76	8.88	7.14	-0.01	-0.22
Turbidity	0.96	1715.00	49.19	6.82	46.98
Colour	2.50	875.00	34.63	6.37	42.45
EC	96.50	48900.00	2569.97	6.17	40.52
TSS	1.00	190.00	17.44	3.70	15.02
TDS	53.10	26895.00	1464.70	6.14	40.17
Na	6.50	13980.00	478.11	6.72	45.98
K	2.00	200.00	14.90	6.65	45.43
Ca	4.00	1540.00	88.46	5.78	36.57
Mg	0.50	1895.00	75.23	6.49	43.68
NH3	0.00	0.82	0.13	1.89	3.56
Cl-	7.90	20249.00	790.73	6.53	44.05
SO42-	3.21	2235.00	135.43	5.76	36.72
PO43-	0.02	3.65	0.32	4.56	22.83
Mn	0.00	0.86	0.12	2.21	4.78
NO2-	0.00	13.00	0.31	6.89	47.59
NO3-	0.01	31.40	9.01	1.25	0.95
F-	0.01	3.27	0.58	1.80	3.69
HCO3-	17.10	525.00	133.65	1.81	3.30

3.2 Correlation Analysis of Hydrochemical Parameters

To further understand the interactions and possible sources of solutes within the groundwater system, a correlation heatmap matrix was generated for all measured hydrochemical parameters based on 50 groundwater samples (Figure X). Electrical Conductivity (EC) showed a strong positive correlation with TDS (r = 0.98), Na^+ (r = 0.96), Cl^- (r = 0.93), and SO_3^{2-} (r = 0.93), indicating that these ions are the primary contributors to salinity and total ionic strength in the groundwater. This cluster of variables points to a dominant salinization process that is likely governed by water–rock interaction and possibly prolonged residence time in the aquifer system (Appelo & Postma, 2005; Sulaiman et al., 2024). The strong correlation between EC and Mg^{2+} (r = 0.86) as well as Ca^{2+} (r = 0.42) further supports the influence of silicate weathering or the dissolution of mafic minerals, consistent with the area's underlying geology comprising amphibolites, granitoids, and mafic dyke lithologies (Hirdes et al., 1992; Junner, 1940). Similarly, the exceptionally high correlations between Na^+–Cl^- (r = 0.97) and Na^+–TDS (r = 0.99) suggest a possible halite dissolution or cation exchange process. However, halite is not expected to be abundant in the Birimian terrain. Instead, these associations may reflect anthropogenic influences, including wastewater seepage or agricultural runoff, which tend to elevate Na^+ and Cl^- levels (Akhtar et al., 2021). The high correlation between SO_3^{2-} and Cl^- (r = 0.91) further supports this notion, especially given the proximity of settlements and farming activities in the study area.

pH showed relatively weak correlations with most major ions, with the highest being a mild positive correlation with HCO_3^- (r = 0.35). This suggests that pH variability is not strongly governed by carbonate equilibrium alone and might be buffered by silicate weathering reactions common in granitoid and amphibolite terrains. The moderate positive association between pH and F^- (r = 0.20) may indicate prolonged water–rock interaction, as F^- is typically mobilized under slightly alkaline conditions during feldspar or biotite weathering (Nordstrom & Jenne, 1977). NH_3, NO_3^-, and NO_2^- generally showed weak correlations with most ions but presented modest positive relationships among themselves—NH_3–NO_2^- (r = 0.46) and NO_2^-–NO_3^- (r = 0.31); hinting at partial nitrification pathways within the aquifer. The low correlation between NO_3^- and Cl (r = 0.21) might suggest mixed origins, including localized leaching from domestic sewage or agricultural application of nitrogen-rich fertilizers. These patterns are consistent with the known rural–peri-urban interface in parts of Assin North and Twifo Atti Morkwa (Gibrilla et al., 2010), where agricultural intensification and domestic pit latrines contribute to nutrient loading in shallow aquifers. The strong positive correlations among divalent cations (e.g., Ca^{2+}–Mg^{2+}, r = 0.45) and between Mg^{2+} and other salinity indicators (Mg^{2+}–TDS, r = 0.82; Mg^{2+}–SO_3^{2-}, r = 0.83) suggest that water chemistry in the area is substantially shaped by

geogenic processes such as the weathering of ferromagnesian minerals (e.g., amphiboles, pyroxenes) in mafic and granitoid rocks. The observed mineralogical units, such as hornblende-biotite granitoids, wacke sediments, and interbedded volcaniclastics (see Figure 1), are consistent with the release of Ca^{2+} and Mg^{2+} through silicate hydrolysis. The relatively low correlation of Mn with major cations and anions indicates its mobilization may be more controlled by redox conditions rather than direct geologic dissolution, aligning with the generally reducing nature of deeper groundwater or those influenced by organic matter decomposition.

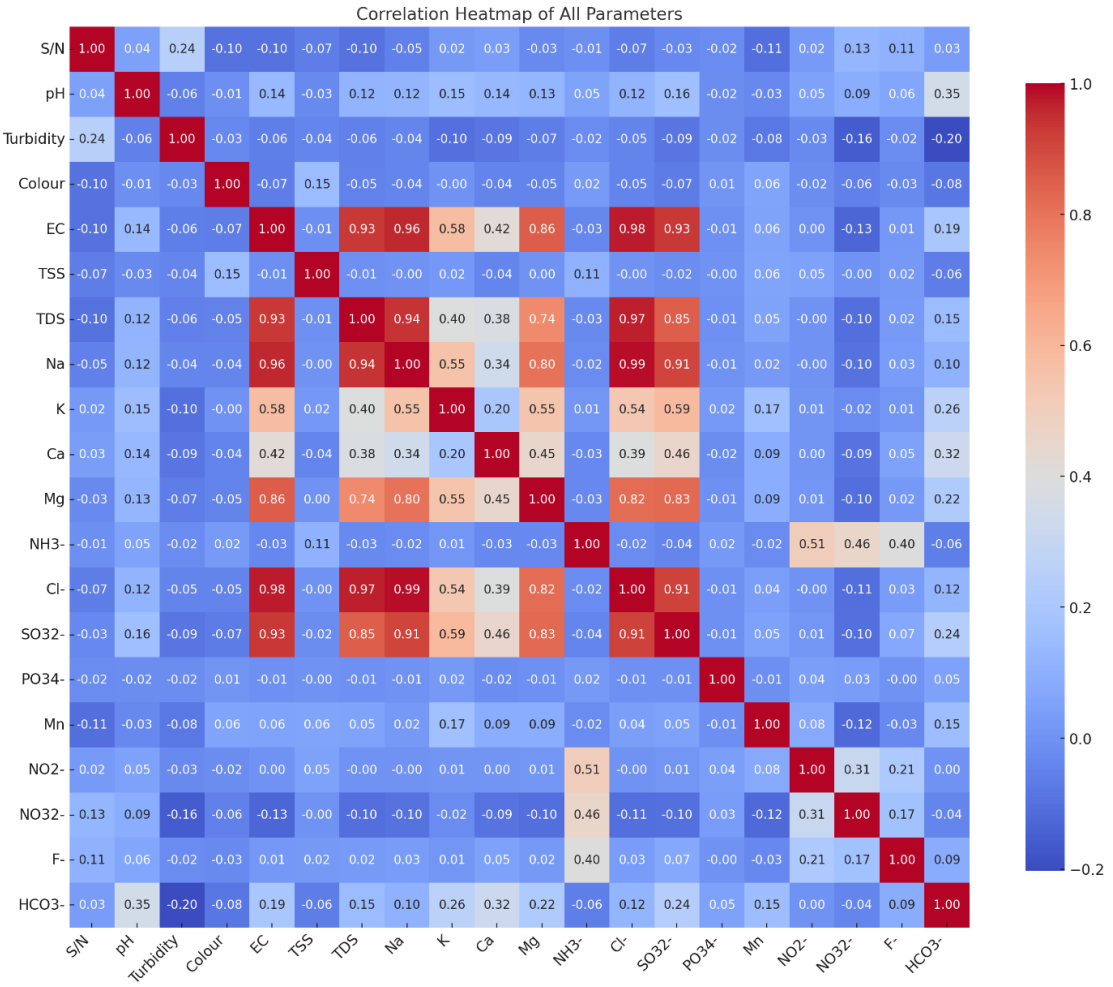

Figure 2: Correlation heatmap of all parameters.

3.3 Hydrogeochemical classification of the groundwater

To discern the underlying processes influencing groundwater chemistry in the transition zone between the Western and Central Regions of Ghana, Principal Component Analysis (PCA) was applied to normalized groundwater quality data collected from the 48 sampling points across both the wet and dry seasons. Following varimax rotation, PCA extracted seven components with eigenvalues greater than 1,

accounting for a cumulative 87.46% of the total variance (Tables 5 & 6). This satisfies Kaiser's criterion (Kaiser, 1960), which retains factors with eigenvalues exceeding unity as statistically meaningful. The rotated solution improved factor interpretability by minimizing cross-loadings (Kazapoe et al., 2025), thus allowing clearer attribution of geochemical processes.

Component 1 alone explained 38.02% of the variance and showed strong positive loadings for Na^+ (0.993), Cl^- (0.993), EC (0.985), TDS (0.985), Mg^{2+} (0.988), K^+ (0.978), and SO_4^{2-} (0.966) (Table 2). These parameters are classical indicators of salinity and total ionic load in groundwater systems and likely represent a dominant geogenic process, particularly rock–water interaction (Appelo & Postma, 2005). The strong co-loading of Na^+ and Cl^- suggests contributions from halite dissolution or weathering of sodic plagioclase feldspars, consistent with the Birimian metavolcanic and granitic lithologies of the study area (Junner, 1940; Hirdes et al., 1992). The presence of Mg^{2+} and SO_4^{2-} may additionally reflect oxidation of sulfide minerals, such as pyrite or marcasite, particularly in mining-dominated zones like Tarkwa-Nsuaem, known for sulfide-rich ore bodies (Kazapoe et al., 2023). The high loading of EC and TDS consolidates the view that this factor represents the overall mineralization status of the groundwater, driven by prolonged residence time, weathering, and ion exchange processes (Ganyaglo et al., 2012; Yidana et al., 2008). Component 2 accounted for 11.06% of the variance and was marked by near-perfect loadings for Turbidity (0.980) and Colour (0.993). These parameters are typically influenced by surface water infiltration, colloidal transport, and suspended particulates, which could be attributed to inadequate well protection, especially in shallow hand-dug wells. The high values in turbidity and colour may reflect inputs of iron/manganese oxides, organic matter, and particulate-bound contaminants, especially during the rainy season or in zones with lateritic cover and sloped terrain, such as parts of Wassa Amenfi East and Twifo Atti Morkwa. This component emphasizes aesthetic quality and physical clarity, suggesting localized surface-groundwater interaction or poor sanitary protection (Kazapoe et al., 2023).

The third component (9.43%) featured strong loadings for HCO_3^- (0.813), Ca^{2+} (0.744), and F^- (0.634). These ions are commonly associated with carbonate mineral dissolution and silicate weathering processes that release bicarbonate into the aquifer. The presence of Ca^{2+} supports the notion of calcite or dolomite dissolution, while F^- is often released from fluorapatite and micas, both typical of granitic terrains in the Birimian Supergroup. The moderate loading of pH (0.361) further suggests a link to alkaline buffering, wherein bicarbonate acts to neutralize acidity. This component likely represents the carbonate-silicate weathering regime and reflects the system's acid-neutralizing capacity, a process enhanced in areas with

intermediate residence time and high water–rock interaction (Appelo & Postma, 2005; Gibrilla et al., 2010). Component 4, accounting for 8.57% of the variance, exhibited strong positive loadings for NO_2^- (0.894) and Mn (0.852). This pattern points to subsurface redox conditions, where NO_2^- represents an intermediate in the nitrification–denitrification chain, and Mn suggests reductive dissolution of Mn-oxides. The co-occurrence of these species typically arises in transition zones within aquifers, where oxic and anoxic microenvironments coexist, potentially due to variable recharge conditions and organic matter decomposition (Shrestha & Kazama, 2007). This is particularly relevant in peri-urban zones or agricultural lands, where fertilizer use and latrine leachates influence nitrogen species. Given Mn's sensitivity to redox, this factor likely reflects mixed anthropogenic and geochemical control.

The fifth component (7.66%) was dominated by PO_4^{3-} (0.881) and moderately by pH (0.579). PO_4^{3-} is widely acknowledged as a marker of anthropogenic contamination, primarily from fertilizers, detergents, and domestic effluents. Its association with pH may reflect phosphate mobility, which is highly pH-dependent, typically increasing under acidic to neutral conditions (Sulaiman et al., 2024). The co-loading suggests localized anthropogenic input superimposed on natural geochemical controls, particularly in settlements and farming zones such as Twifo Atti Morkwa and Assin North. This component showed a dominant loading for Total Suspended Solids (TSS = 0.891), explaining 6.52% of the total variance. TSS primarily indicates particulate content, which may originate from poor well construction, surface infiltration, or incomplete filtration in shallow wells. While it overlaps with Component 2 (turbidity/colour), its separation here suggests that not all suspended material affects turbidity uniformly, and that TSS may also reflect mineral fines or biological flocs, especially during recharge events.

The final component (6.20%) revealed high loadings for NO_3^- (0.819) and NH_3 (0.647). This signature aligns strongly with anthropogenic pollution, particularly fertilizer application, septic leakage, and organic waste decomposition. The simultaneous presence of NH_3 (a reduced form) and NO_3^- (an oxidized form) underscores varying redox conditions, which could exist across shallow unconfined aquifers or due to intermittent flushing and recharge (Shrestha & Kazama, 2007). This component further highlights the vulnerability of the aquifer system to land-use practices, particularly in agricultural and semi-urban settings.

Table 5: Total Variance Explained

Component	Initial Eigenvalues			Extraction Sums of Squared Loadings			Rotation Sums of Squared Loadings		
	Total	% of Variance	Cumulative %	Total	% of Variance	Cumulative %	Total	% of Variance	Cumulative %
1	7.581	39.897	39.897	7.581	39.897	39.897	7.223	38.017	38.017
2	2.302	12.117	52.014	2.302	12.117	52.014	2.101	11.055	49.073
3	1.891	9.951	61.966	1.891	9.951	61.966	1.792	9.432	58.505
4	1.537	8.091	70.056	1.537	8.091	70.056	1.628	8.569	67.074
5	1.205	6.343	76.399	1.205	6.343	76.399	1.456	7.661	74.735
6	1.093	5.754	82.153	1.093	5.754	82.153	1.238	6.516	81.251
7	1.007	5.301	87.455	1.007	5.301	87.455	1.179	6.204	87.455
8	0.727	3.828	91.282						
9	0.653	3.435	94.717						
10	0.427	2.248	96.965						
11	0.297	1.562	98.527						
12	0.204	1.076	99.603						
13	0.046	0.244	99.846						
14	0.011	0.057	99.903						
15	0.010	0.053	99.956						
16	0.004	0.023	99.979						
17	0.003	0.018	99.997						
18	0.000	0.002	100.000						
19	7.160E-05	0.000	100.000						

Extraction Method: Principal Component Analysis.

Table 6: Rotated Component Matrix[a]

	Component						
	1	2	3	4	5	6	7
pH	0.361	-0.180	0.155	-0.240	**0.579**	-0.216	-0.122
Turbidity	-0.017	**0.980**	-0.057	-0.022	-0.023	0.002	-0.038
Colour	-0.037	**0.993**	-0.038	-0.043	-0.029	0.023	0.009
EC	**0.985**	-0.030	0.121	0.019	0.034	0.027	-0.054
TSS	0.111	0.011	-0.057	0.000	-0.006	**0.891**	-0.046
TDS	**0.985**	-0.033	0.119	0.021	0.031	0.022	-0.043
Na	**0.993**	-0.010	0.059	-0.023	0.025	0.027	-0.026
K	**0.978**	0.003	0.016	-0.055	0.080	0.056	-0.018
Ca	0.205	0.026	**0.744**	-0.055	-0.168	-0.208	-0.083
Mg	**0.988**	-0.018	0.081	-0.001	0.030	0.024	-0.050
NH3	-0.122	0.238	-0.106	-0.072	-0.306	0.340	**0.647**
Cl-	**0.993**	-0.016	0.090	0.000	0.015	0.027	-0.039
SO_4^{2-}	**0.966**	-0.022	0.185	0.014	0.058	-0.024	-0.060
PO_4^{3-}	-0.014	0.040	-0.017	-0.032	**0.881**	0.062	0.101
Mn	-0.029	-0.086	0.185	**0.852**	-0.119	0.235	-0.132
NO_2^-	0.028	0.006	-0.111	**0.894**	-0.023	-0.196	0.057
NO_3^-	-0.070	-0.179	-0.057	-0.012	0.230	-0.232	**0.819**
F^-	0.487	-0.103	**0.634**	0.169	-0.076	0.282	0.096
HCO_3^-	0.023	-0.102	**0.813**	0.030	0.365	0.008	-0.103

Rotation Method: Varimax with Kaiser Normalization.

a. Rotation converged in 6 iterations

The dendrogram generated using Ward's linkage method (Figure 3) provides a structured view of the relationships among 19 hydrochemical parameters from groundwater samples in the study area. The tightest cluster, forming at the lowest rescaled distance, comprises electrical conductivity (EC), total dissolved solids (TDS), and chloride (Cl^-). These parameters exhibit a strong positive association and are primary indicators of groundwater mineralization, reflecting the ionic load and salinity status of aquifer systems (Freeze & Cherry, 1979). EC and TDS are particularly sensitive to rock–water interactions, solute accumulation, and residence time. At the same time, Cl^- often functions as a conservative tracer, suggesting minimal reactivity and highlighting either natural halite dissolution or septic return flows (Appelo & Postma, 2005). The tight coalescence of these parameters in the dendrogram underscores their shared origin in deep circulation pathways and mineralized zones such as those found in Tarkwa-Nsuaem and Wassa Amenfi East, where sulfide-rich and granitic lithologies dominate (Hirdes et al., 1992; Junner, 1940). The second, broader cluster binds Na^+, Mg^{2+}, SO_4^{2-}, Ca^{2+}, HCO_3^-, and, to a lesser extent, potassium

(K^+). This group represents a hydrogeochemical suite indicative of silicate weathering, carbonate dissolution, and possible cation exchange processes typical of groundwater in fractured crystalline and metamorphic terrains (Appelo & Postma, 2005). The clustering of HCO_3^- with divalent cations (Ca^{2+} and Mg^{2+}) suggests a dominant control from carbonate equilibria, consistent with the dissolution of calcite, dolomite, or weathered plagioclase feldspars in the Birimian Supergroup. SO_4^{2-} in this group may arise from oxidation of sulfide minerals such as pyrite, a common feature in the mining belts of Tarkwa (Kazapoe et al., 2023).

The presence of Na^+ and K^+ may reflect feldspar alteration or minor anthropogenic inputs, particularly from agricultural return flows or domestic leachates. This cluster supports a geogenic signature, heavily shaped by bedrock composition, aquifer residence time, and regional lithological diversity. The most dispersed cluster, merging at higher rescaled distances, includes Mn, NO_2^-, NO_3^-, NH_3, PO_4^{3-}, F^-, pH, colour, and turbidity. This assemblage suggests a mixed control involving redox processes, nutrient dynamics, and surface-related anthropogenic inputs. The close grouping of oxidized (NO_3^-) and reduced (NH_3, NO_2^-) nitrogen species points to spatial redox heterogeneity in the aquifer, likely driven by organic loading, variable recharge, and inconsistent sanitation infrastructure in peri-urban and agricultural zones such as Twifo Atti Morkwa and Assin North (Shrestha & Kazama, 2007). Mn, often mobilized under anoxic conditions, further corroborates reductive dissolution processes occurring in organically enriched aquifers (Appelo & Postma, 2005). The inclusion of PO_4^{3-} and F^- in this group may reflect both geogenic and anthropogenic origins. Fluoride is typically derived from fluorite-bearing rocks and biotite micas, while phosphate is linked to fertilizer leaching, detergent runoff, and latrine seepage. Their co-occurrence with pH, turbidity, and colour highlights the sensitivity of groundwater to land use and sanitary conditions, particularly in shallow aquifers with unprotected wellheads. The dispersed nature of this cluster suggests that localized environmental factors (e.g., infiltration, erosion, and land use intensity) significantly modulate the chemistry of these parameters.

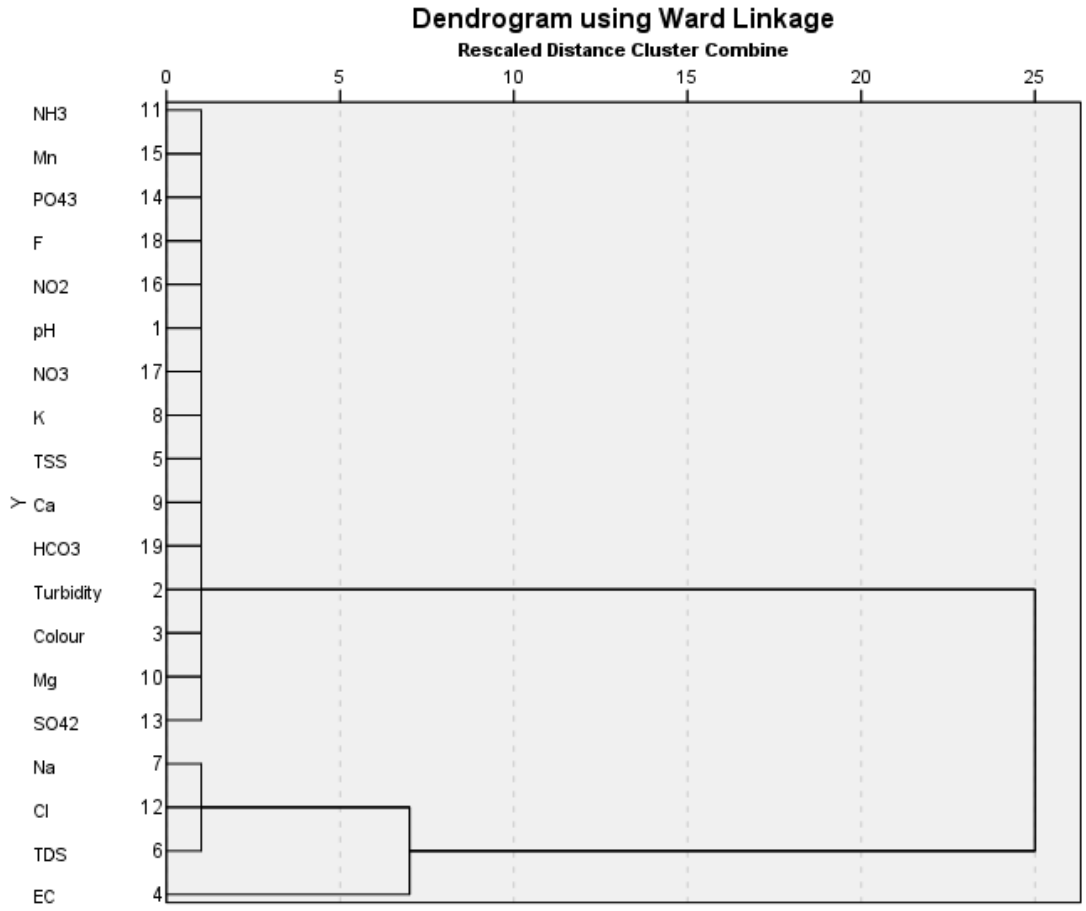

Figure 3: Dendrogram from R-mode HCA describing groundwater quality.

To better understand the geochemical evolution of groundwater in the transition zone between the Western and Central Regions of Ghana, a suite of bivariate ion plots was employed to investigate dominant mineral weathering processes. Figure 4a presents a scatter plot of bicarbonate (HCO_3^-) versus the sum of calcium and magnesium ions ($Ca^{2+} + Mg^{2+}$), both in milliequivalents per litre (meq/L). Theoretical 1:1 stoichiometric lines are included (dashed red) to assess the proportionality between these ions. The majority of groundwater samples are clustered in the lower concentration ranges (i.e., < 25 meq/L), consistent with natural groundwater systems. However, most of these points lie significantly below the 1:1 line, indicating that bicarbonate concentrations are substantially lower than those of Ca^{2+} and Mg^{2+}. This pattern diverges from typical silicate weathering signatures, where HCO_3^- tends to dominate due to carbonic acid-driven mineral dissolution (Appelo & Postma, 2005). Instead, the excess of Ca^{2+} and Mg^{2+} over HCO_3^- suggests significant contributions from non-bicarbonate sources, such as the dissolution of gypsum, evaporites, or acid mine drainage processes potentially linked to extensive artisanal and large-scale gold mining activities in the region (Kortatsi, 2007; Ganyaglo et al.,

2012). Further evidence of the anomalous cationic composition is seen in Figure 4b, which compares Ca^{2+} + Mg^{2+} to total cations (TZ^{+}).

Under ideal conditions dominated by carbonate or silicate weathering, a strong linear alignment near the 1:1 line is expected, reflecting a balanced contribution of divalent cations to total ionic strength (Gibbs, 1970; Garrels & Mackenzie, 1971). However, in this case, the majority of samples fall well below the 1:1 line, revealing that Ca^{2+} and Mg^{2+} comprise only a fraction of the total cation load. This supports the view that alkali metals such as Na^{+} and K^{+}, likely sourced from feldspar and mica weathering, or ion exchange processes in the aquifer matrix, contribute significantly to the groundwater chemistry (Datta & Tyagi). In regions like Tarkwa and Wassa, where lateritic soils overlie weathered granitoid rocks, base cation enrichment from feldspar decay is a common hydrochemical signature (Kazapoe et al., 2023). Figure 4c displays HCO_3^{-} + SO_4^{2-} plotted against Ca^{2+} + Mg^{2+}. This diagnostic plot distinguishes between dominant weathering pathways, with the 1:1 equiline serving as a threshold: data points falling above the line imply silicate weathering dominance, while those below suggests carbonate dissolution (Stallard & Edmond, 1983). However, in this case, most samples again lie below the equiline, reinforcing the interpretation that carbonate weathering and possibly anthropogenic sulfate inputs (e.g., from mine tailings or fertilizers) play a key role in shaping water chemistry. The prevalence of low bicarbonate relative to Ca^{2+} + Mg^{2+}, in conjunction with elevated sulfate in some samples, suggests influence from sulfide oxidation processes, an expected phenomenon in sulfide-rich terrains such as Tarkwa and Prestea (Kuma & Younger, 2001).

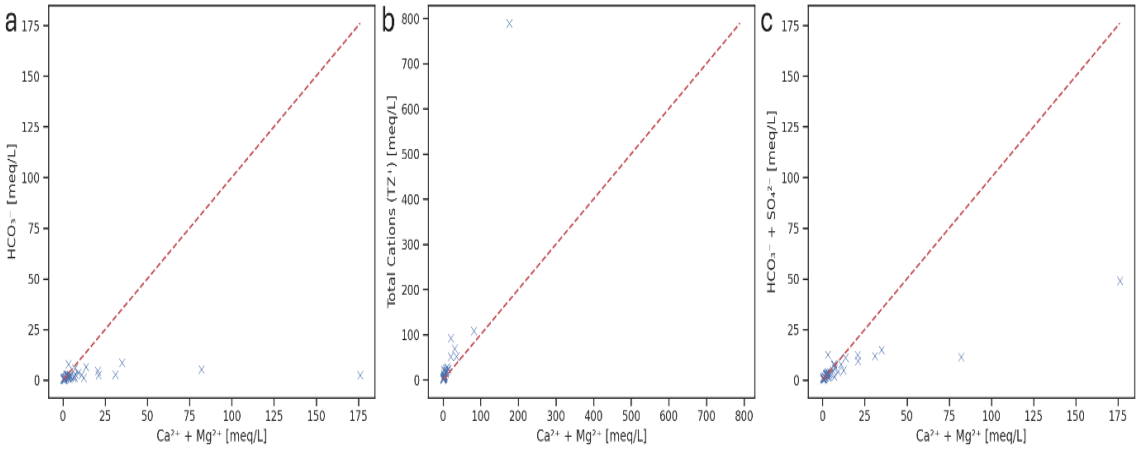

Figure 4: Figure showing (a) A plot of HCO3- against Ca + Mg (b) A plot of total cations against Ca + Mg (c) A plot of HCO3- + SO42+ against Ca + Mg.

The Piper diagram (Figure 5) reveals distinct groundwater hydrochemical facies across the Wassa Amenfi East, Tarkwa-Nsuaem, Twifo Atti Morkwa, and Assin North districts based on 50 groundwater samples analysed for major cations and anions. In the cation field, the chemistry is dominated by alkaline earth metals, with 78% of samples falling in the Ca^{2+}–Mg^{2+} zone and 45% showing calcium dominance, likely sourced from the weathering of plagioclase and amphibole minerals in the Birimian rocks (Hirdes et al., 1992; Gibrilla et al., 2011). The anion field shows a strong presence of chloride and sulphate, with over 60% of samples plotting toward the Cl^- + F^- and SO_4^{2-} apices. This suggests anthropogenic input and sulphide oxidation, especially in mining-impacted zones like Tarkwa (Kuma & Younger, 2017; Ganyaglo et al., 2012). Sodium-potassium enrichment is minimal, indicating limited sodic alteration or brief water–rock interaction, possibly due to low residence times or the absence of extensive cation exchange with clayey saprolites (Freeze & Cherry, 1979; Domenico & Schwartz, 1997. In the combined diamond field, 66% of samples fall within the Ca–Mg–Cl–SO_4 facies, commonly found in valley-bottom and mineralised zones with extended residence time and intensive water–rock interaction (Appelo & Postma, 2005). These are particularly prevalent in Tarkwa-Nsuaem and southern Wassa, aligning with mafic and sediment-rich geological formations (Figure 1). Around 20% of the samples belong to the Ca–Mg–HCO_3 facies, representing fresher, less-evolved groundwater, likely sourced from upland recharge zones in Assin North and Twifo Atti Morkwa. These areas are characterized by limited anthropogenic activity and dominant silicate weathering (Gibrilla et al., 2010; National Research Council, 1996). Less than 10% of samples show a shift toward Na–Cl or Na–HCO_3 facies, consistent with low salinity conditions and short flow paths supported by the region's high rainfall and shallow aquifers.

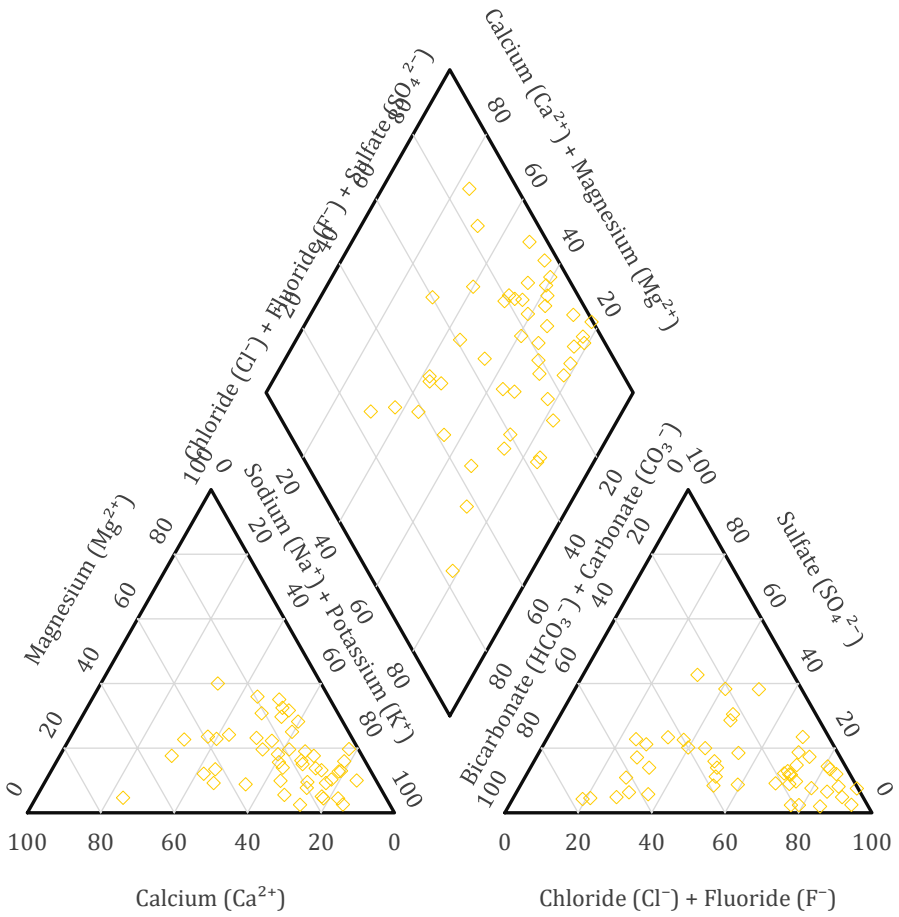

Figure 5: Diamond plot of groundwater in the area.

3.4 Groundwater Suitability for Irrigation

To assess the suitability of groundwater for irrigation purposes in the study area, a suite of hydrochemical indices was evaluated: Residual Sodium Bicarbonate (RSBC), Sodium Adsorption Ratio (SAR) and Permeability Index (PI) as shown in Table 7. The distribution of Na% indicates a significant sodicity risk across the study area. While 16.67% of samples fell into the 'Good' class (Na% 20–40%), and 29.17% were 'Permissible' (Na% 40–60%), a striking 43.75% of the samples were 'Doubtful' (Na% 60–80%), and 10.42% were 'Unsuitable' (Na% >80%). Elevated Na% values are known to deteriorate soil structure by causing clay particle dispersion, which reduces permeability, water infiltration, and aeration (Wilcox, 1955). In agrarian communities such as Wassa Amenfi East and Twifo Atti Morkwa, where cocoa and staple crops dominate, the long-term use of sodic groundwater for irrigation could result in soil hardening, nutrient imbalance, and reduced crop productivity. The mild positive skew (0.56) and near-mesokurtic distribution (–0.29) for this group point to a relatively consistent presence of sodium-enriched groundwater across the area. This pattern is consistent with ion-exchange reactions and weathering of feldspathic

rocks, known to release Na^+ into groundwater in the Birimian belt (Ganyaglo et al., 2012).

SAR values varied widely across the samples, reflecting diverse geochemical regimes. Approximately 29.17% of the samples were classified as "Good" (SAR 10–18), and 25.0% fell within the "Doubtful" range (SAR 18–26), while 16.67% were "Excellent" (SAR <10). However, a notable 29.17% of samples had SAR values >26, deemed "Unsuitable." This group had a mean SAR of 77.48, with an extreme maximum value of 412.61 and a very high standard deviation (SD = 100.12), indicating the influence of intense local contamination or evaporative concentration. The extreme positive skew (2.95) and leptokurtic nature (7.43) suggest highly heterogeneous conditions, potentially linked to anthropogenic input, including tailings or poor irrigation return flows (Richards, 1954). These findings point to potential long-term sodicity hazards that could compromise agricultural productivity.

All samples exceeded the RSBC threshold of 2.50, indicating widespread unsuitability for irrigation. A dominant 87.5% of samples were classified as "Excellent" under the RSBC classification (RSBC > 2.5), though this label is technically misleading, as the high RSBC signifies high bicarbonate relative to calcium—a condition conducive to calcium carbonate precipitation and subsequent soil degradation (Gupta & Gupta, 1987). The remaining 12.5% of samples were anomalously negative (RSBC < 0), with a mean of –251.87 and an extremely high standard deviation (SD = 480.43). The bimodal nature—marked by high positive and extreme negative RSBC values, suggests competing hydrochemical processes: bicarbonate enrichment on one hand, and calcium dominance in others, possibly from carbonate rock dissolution. The presence of such extreme values, with skewness (–1.64) and platykurtic characteristics, points to unstable water–rock interaction processes, possibly intensified by anthropogenic inputs or seasonal dilution.

The PI analysis classified groundwater into three main irrigation suitability classes: 12.5% "Excellent" (PI < 50), 58.33% "Good" (50–75), and 29.17% "Permissible" (75–100). The bulk of samples fell within acceptable limits, with a mean PI of 65.40 for the "Good" category. The standard deviation (SD = 5.73) and slight negative skew (–0.21) suggest low dispersion and a relatively symmetric distribution. However, 29.17% of samples in the upper PI range (mean = 82.31) reflect increasing bicarbonate and sodium contributions, likely affecting permeability over time (Doneen, 1964). While all samples remain within the broadly suitable range for irrigation, increasing PI values should be monitored, particularly in low-permeability soils.

3.5 Groundwater Pollution Indices

To further assess the quality and potential health risks associated with groundwater in the study area, three pollution indices were computed. These are Pollution Index of Groundwater (PIG), Fluoride Pollution Index (FPI), and Nitrate Pollution Index (NPI), as shown in Table 8. These indices integrate multiple hydrochemical parameters and compare them against established drinking water standards, providing a nuanced assessment of contamination severity and its implications for human and environmental health.

The NPI values indicate that 89.58% of the groundwater samples are within safe nitrate levels, classified as "Moderate" (NPI –1 to 0), with a mean of –0.66. This is consistent with the geochemical attenuation expected in a tropical weathering profile, where denitrification processes and limited anthropogenic loading prevail (Rivett et al., 2008). However, 10.42% of the samples fell into the "Polluted" category (NPI 0–1), with values as high as 0.57, suggesting localized nitrate enrichment. This likely results from surface contamination sources such as agricultural runoff or unlined sanitation facilities. The slight negative skew (–0.73) and low standard deviation (SD = 0.21) within this group indicate constrained but significant nitrate risk hotspots that warrant localized mitigation.

The Fluoride Pollution Index (FPI) revealed varying levels of risk, with values ranging from 1.00 to 3.25. A total of 62.5% of the samples fell within the "Low" category (FPI ≤ 2), suggesting minimal combined fluoride-related hazards for most of the groundwater (mean = 1.76; SD = 0.25). However, 35.42% of the samples were classified as "Medium" (FPI 2–3), and one sample (2.08%) exceeded an FPI of 3, categorized as "High." The presence of even a single high-risk zone is ecologically important, as chronic fluoride exposure is cumulative and may have long-term health implications (Kazapoe et al., 2024). The positive skewness (0.50) for the medium-risk class and the platykurtic shape (–1.19) suggest moderate variability with some influence from localized geochemical conditions, likely linked to silicate weathering and bicarbonate enrichment typical of granitic terrains.

The PIG results reveal significant variability in groundwater quality. While 58.33% of the samples were classified as "Low" pollution risk (PIG ≤ 1), 16.67% were "Medium" (PIG 1–2), and 25.0% were "High" (PIG > 2), with some values reaching as high as 21.92. The "High" pollution group had a mean of 5.72. It showed strong positive skew (1.77) and moderate kurtosis (1.24), pointing to localized degradation likely driven by anthropogenic pressures such as small-scale mining, domestic waste, and inadequate wastewater infrastructure (Ravikumar et al., 2011). These values reflect a mosaic of hydrogeological vulnerabilities, necessitating site-specific interventions.

Although the present study reflects a snapshot in time, groundwater quality in the region is strongly influenced by seasonal dynamics. The bimodal rainfall regime produces marked wet and dry season contrasts in recharge and geochemical conditions. During the wet season, enhanced infiltration facilitates flushing of nitrates, agrochemicals, and mine-derived solutes into aquifers, especially shallow wells. Conversely, during the dry season, reduced recharge and higher evapotranspiration intensify salinity, bicarbonate accumulation, and mobilization of fluoride from weathered granitoids. Previous hydrogeochemical studies in southern Ghana have documented seasonal fluctuations in redox-sensitive parameters such as iron and manganese as well as nitrate levels (Ganyaglo et al., 2012; Dorleku et al., 2019). These patterns highlight the importance of integrating seasonal monitoring into future groundwater assessments to provide a more complete understanding of temporal variability.

Table 8: Summary of irrigation suitability and pollution indices of the groundwater samples

	Index	Class	Percentage	Mean	Min	Max	Mean
1.	FPI_Class	High (>3)	2.08	3.25	3.25	3.25	3.25
2.	FPI_Class	Low (≤2)	62.50	1.76	1.00	2.00	1.76
3.	FPI_Class	Medium (2-3)	35.42	2.53	2.25	3.00	2.53
4.	Na%_Class	Doubtful (60-80%)	43.75	66.54	60.23	75.75	66.54
5.	Na%_Class	Good (20-40%)	16.67	33.83	26.62	39.71	33.83
6.	Na%_Class	Permissible (40-60%)	29.17	53.02	44.35	58.82	53.02
7.	Na%_Class	Unsuitable (>80%)	10.42	83.48	80.50	86.64	83.48
8.	SAR_Class	Doubtful (18-26)	25.00	22.58	18.42	25.95	22.58
9.	SAR_Class	Excellent (<10)	16.67	6.34	3.13	9.10	6.34
10.	SAR_Class	Good (10-18)	29.17	13.41	10.03	17.15	13.41
11.	SAR_Class	Unsuitable (>26)	29.17	77.48	27.00	412.61	77.48
12.	RSBC_Class	Excellent (>2.5)	87.50	87.63	9.10	463.90	87.63
13.	RSBC_Class	Unsuitable (<0)	12.50	-251.87	-1213.00	-3.80	-251.87
14.	PI_Class	Excellent (<50)	12.50	41.80	27.45	49.08	41.80
15.	PI_Class	Good (50-75)	58.33	65.40	53.90	74.87	65.40
16.	PI_Class	Permissible (75-100)	29.17	82.31	75.22	94.50	82.31
17.	NPI_Class	Moderate (-1 to 0)	89.58	-0.66	-1.00	-0.06	-0.66
18.	NPI_Class	Polluted (0-1)	10.42	0.38	0.06	0.57	0.38
19.	PIG_Class	High (>2)	25.00	5.72	2.04	21.92	5.72
20.	PIG_Class	Low (≤1)	58.33	0.60	0.21	0.98	0.60
21.	PIG_Class	Medium (1-2)	16.67	1.29	1.06	1.50	1.29

4 Conclusion and Recommendation

This study conducted a comprehensive hydrogeochemical characterization of groundwater in parts of the Western and Central Regions of Ghana, focusing on 48 samples collected from the Wassa Amenfi East, Tarkwa-Nsuaem, Twifo Atti Morkwa, and Assin North districts. The results revealed considerable spatial variation in groundwater quality, shaped by both geogenic and anthropogenic processes. While most parameters such as NO_3^-, HCO_3^-, and PO_4^{3-} remained within safe thresholds, elevated concentrations of TDS, EC, Na^+, Cl^-, SO_4^{2-}, and certain trace elements (e.g., Mn, F^-) were recorded in a subset of samples, particularly near mining and agricultural zones. Water types were predominantly of the Ca–Mg–Cl–SO_4 facies, indicating strong influence from mineralized bedrock and evaporative enrichment. Multivariate analyses (PCA and HCA) identified key processes including water–rock interaction, silicate and carbonate weathering, redox-driven mobilization of nutrients and metals, and surface-derived contamination. Although majority of samples were suitable for domestic and irrigation purposes based on SAR, Na%, and PI classifications, the RSBC index flagged widespread unsuitability for irrigation due to excess bicarbonate and low calcium levels. Pollution indices (PIG, FPI, NPI) highlighted localized hotspots of nitrate and fluoride contamination, underscoring the vulnerability of groundwater to land-use practices and inadequate sanitation.

Based on the above, here are some recommendations.

- National and local regulatory bodies, including the Water Resources Commission (WRC), Environmental Protection Agency (EPA–Ghana), Ghana Water Company Limited (GWCL), District Assemblies, and the Community Water and Sanitation Agency (CWSA), should map areas vulnerable to groundwater contamination, especially near mining and farming zones. These agencies should also institute regular monitoring of key pollutants such as fluoride, nitrate, salinity, and trace metals. The Environmental Protection Agency (EPA–Ghana), Minerals Commission, and Ministry of Food and Agriculture (MoFA) should lead in enforcing environmental laws on mining and agriculture, particularly in managing mine tailings, effluents, and agrochemical use. Their efforts should be complemented by District Assemblies and traditional authorities, who can ensure compliance at the community level through local monitoring and sensitization.
- The Community Water and Sanitation Agency (CWSA), District Assemblies, and EPA–Ghana, in partnership with NGOs and traditional leaders, should coordinate public awareness campaigns to encourage safe waste and fertilizer use, alongside upgrading poorly constructed wells to prevent contamination.

- The Ministry of Food and Agriculture (MoFA) through its extension services should promote low-impact agricultural methods such as organic fertilizers, cover cropping, and buffer zones near water bodies.
- The Water Resources Commission (WRC), Lands Commission, and District Assemblies should ensure that land-use policies are tailored to aquifer characteristics by mapping recharge zones and restricting harmful activities in sensitive areas.
- Long-term studies on seasonal changes and redox conditions (e.g., Mn, Fe, NO_2^-) should be undertaken by universities and research institutions, including CSIR–Water Research Institute, in collaboration with WRC and EPA, to strengthen groundwater quality management.

5 Funding

The author received no specific funding for this work.

6 Conflicts of interest/Competing interests

The author declares no known competing interest

7 Availability of data and material

Not applicable

8 Code availability

Not applicable

References

Abanyie, S. K., Ampofo, S., Douti, N. B., & Boateng, T. (2018). Geospatial Assessment of Groundwater Quality in the Savelugu-Nanton Municipality, Northern Ghana. African Journal of Applied Research, 4(1), 93-105.

Akhtar, N., Syakir Ishak, M. I., Bhawani, S. A., & Umar, K. (2021). Various natural and anthropogenic factors responsible for water quality degradation: A review. Water, 13(19), 2660.

Akoto, O., Teku, J. A., & Gasinu, D. (2019). Chemical characteristics and health hazards of heavy metals in shallow groundwater: Case study Anloga community, Volta Region, Ghana. Applied Water Science, 9(2), 36. https://doi.org/10.1007/s13201-019-0916-9

Akurugu, B. A., Chegbeleh, L. P., & Yidana, S. M. (2020). Characterisation of groundwater flow and recharge in crystalline basement rocks in the Talensi District, Northern Ghana. Journal of African Earth Sciences, 161, 103665.

American Public Health Association (APHA). (1998). Standard methods for the examination of water and wastewater (21st ed., p. 1378). American Water Works Association/Water Environment Federation.

American Public Health Association (APHA). (2017). Standard methods for the examination of water and wastewater. In American Public Health Association.

Amuah, E. E. Y., Boadu, A. J., & Nandomah, S. (2022). Emerging issues and approaches to protecting and sustaining surface and groundwater resources: Emphasis on Ghana. Groundwater for Sustainable Development, 16, 100705. https://doi.org/10.1016/j.gsd.2021.100705

Appelo, C. A. J., & Postma, D. (2005). Geochemistry, groundwater and pollution (2nd ed.). CRC Press.

Bekoe, E. M. O., Amuah, E. E. Y., Abuntori, Z. N., Sintim, E., Kichana, E., & Quarcoo, G. (2021). Water quality impacts from the multipurpose use of the Golinga Reservoir in northern Ghana. Water, Air & Soil Pollution, 232(9), 1–15. https://doi.org/10.1007/s11270-021-05306-3

Buamah, R., Petrusevski, B., & Schippers, J. C. (2008). Presence of arsenic, iron and manganese in groundwater within the gold-belt zone of Ghana. Journal of Water Supply: Research and Technology—AQUA, 57(7), 519–529. https://doi.org/10.2166/aqua.2008.086

Datta, P. S., & Tyagi, S. K. (1996). Major ion chemistry of groundwater in Delhi area: chemical weathering processes and groundwater flow regime. Journal geological society of India, 47(2), 179-188.

Dickson, K. B., & Benneh, G. (1988). A new geography of Ghana. Longman.

Domenico, P. A., & Schwartz, F. W. (1997). Physical and chemical hydrogeology. John wiley & sons.

Doneen, L. D. (1964). Notes on water quality in agriculture (Water Science and Engineering Paper 4001). Department of Water Science and Engineering, University of California.

Dorleku, M. K., Affum, A. O., Tay, C. K., & Nukpezah, D. (2019). Assessment of nutrients levels in groundwater within the Lower Pra Basin of Ghana. Ghana Journal of Science, 60(1), 24–36.

Douti, N. B., Amuah, E. E. Y., Abanyie, S. K., & Amanin-Ennin, P. (2021). Irrigation water quality and its impact on the physicochemical and microbiological contamination of vegetables produced from market gardening: A case of the Vea Irrigation Dam, UER, Ghana. Journal of Water and Health, 19(2), 203–215. https://doi.org/10.2166/wh.2021.217

Freeze, R. A., & Cherry, J. A. (1979). Groundwater. Prentice Hall.

Garrels, R. M., & Mackenzie, F. T. (1971). Evolution of sedimentary rocks. New York, NY: W. W. Norton and Company.

Ganyaglo, S. Y., Banoeng-Yakubo, B., Osae, S., Dampare, S. B., Fianko, J. R., & Bhuiyan, M. A. (2010). Hydrochemical and isotopic characterisation of groundwaters in the eastern region of Ghana. Journal of water resource and protection, 2(3), 199-208.

Ganyaglo, S.Y., Osae, S., Dampare, S.B., Fianko, J.R., Bhuiyan, M.A., Gibrilla, A., Bam, E., Ahialey, E. and Osei, J. (2012). Preliminary groundwater quality assessment in the central region of Ghana. Environmental Earth Sciences, 66, pp.573-587.

Gibbs, R. J. (1970). Mechanisms controlling world water chemistry. Science, 170(3962), 1088-1090.

Gibrilla, A., Akiti, T. T., Osae, S., Adomako, D., Ganyaglo, S. Y., Bam, E. P. K., & Hadisu, A. (2010). Hydrogeochemical and groundwater quality studies in the northern part of the Densu River Basin of Ghana. Journal of Water Resource and Protection, 2(11), 1071–1081.

Gibrilla, A., Bam, E. K. P., Adomako, D., Ganyaglo, S., Osae, S., Akiti, T. T., Kebede, S., Achoribo, E., Ahialey, E., Ayanu, G., & Agyeman, E. K. (2011). Application of water quality index (WQI) and multivariate analysis for groundwater quality assessment of the Birimian and Cape Coast Granitoid Complex: Densu River Basin of Ghana. Water Quality Exposure and Health, 3(1), 63–78. https://doi.org/10.1007/s12403-011-0044-9

Gupta, S. K., & Gupta, I. C. (1987). Management of saline soils and water (p. 399). Oxford and IBH Publishing Co.

Harris, N. (2007). Channel flow and the Himalayan–Tibetan orogen: a critical review. Journal of the Geological Society, 164(3), 511-523.

Hadzi, G. Y., Essumang, D. K., & Ayoko, G. A. (2018). Assessment of contamination and health risk of heavy metals in selected water bodies around gold mining areas in Ghana. Environmental Monitoring and Assessment, 190(7), 406. https://doi.org/10.1007/s10661-018-6802-0

Hirdes, W., Davis, D. W., & Eisenlohr, B. N. (1992). Reassessment of Proterozoic granitoid ages in Ghana on the basis of single zircon dating. Precambrian Research, 56(1–2), 89–96.

Junner, N. R. (1940). Geology of the Gold Coast and Western Togoland (with revised geological map) (Gold Coast Geological Survey Bulletin No. 11, 40 pp.).

Kaiser, H. F. (1960). The application of electronic computers to factor analysis. Educational and psychological measurement, 20(1), 141-151.

Kazapoe, R. W., Addai, M. O., Amuah, E. E. Y., & Dankwa, P. (2023). Hydrogeochemical characterization of groundwater in the Wassa Amenfi East and Prestea-Huni Valley areas of southern Ghana using GIS-based and multivariate statistical techniques. Sustainable Water Resources Management, 9(5), 141.

Kazapoe, R. W., Addai, M. O., Amuah, E. E. Y., & Dankwa, P. (2024). Characterization of groundwater in southwest Ghana: Implications for sustainable agriculture and safe water supply in a mining-dominated zone. Environmental and Sustainability Indicators, 22, 100341.

Kazapoe, R. W., Kwayisi, D., Alidu, S., Fynn, O. F., Sagoe, S. D., Amuah, E. E. Y., & Nyavor, E. (2025). Patterns and source apportionment of potentially toxic elements distribution in the soils of the Nangodi area, Northeast Ghana: A multivariate and machine learning approach. Journal of Hazardous Materials Advances, 18, 100688.

Kortatsi, B. K. (2007). Groundwater quality in the Wassa West district of the western region of Ghana. West African Journal of Applied Ecology, 11(1).

Kuma, J. S., & Younger, P. L. (2001). Pedological characteristics related to groundwater occurrence in the Tarkwa area, Ghana. Journal of African Earth Sciences, 33(2), 363-376.

Lanjwani, M. F., Khuhawar, M. Y., Jahangir Khuhawar, T. M., Lanjwani, A. H., Jagirani, M. S., Kori, A. H., Muhammad, D. J. (2019). Risk assessment of heavy metals and salts for human and irrigation consumption of groundwater in Qambar city: A case study. Geology, Ecology, and Landscapes, 4(1), 23–39.

Malm, O., Branches, F.J., Akagi, H., Castro, M.B., Pfeiffer, W.C., Harada, M., Bastos, W.R. & Kato, H. (1995). Mercury and methylmercury in fish and human hair from the Tapajos river basin, Brazil. Science of the total Environment, 175(2), pp.141-150.

National Research Council. (1996). Rock fractures and fluid flow: Contemporary understanding and applications. The National Academies Press.

Nordstrom, D. K., & Jenne, E. A. (1977). Fluorite solubility equilibria in selected geothermal waters. Geochimica et Cosmochimica Acta, 41(2), 175-188.

Obiri, S. (2007). Determination of heavy metals in water from boreholes in Dumasi in the Wassa West District of Western Region of Republic of Ghana. Environmental Monitoring and Assessment, 130(1–3), 455–463. https://doi.org/10.1007/s10661-006-9435-y

Olayinka, O. O., Akande, O. O., Bamgbose, K., & Adetunji, M. T. (2017). Physicochemical characteristics and heavy metal levels in soil samples obtained from selected anthropogenic sites in Abeokuta, Nigeria. Journal of Applied Sciences and Environmental Management, 21(5), 883–891.

Owusu-Nimo, F., Mantey, J., Nyarko, K. B., Appiah-Effah, E., & Aubynn, A. (2018). Spatial distribution patterns of illegal artisanal small scale gold mining (Galamsey) operations in Ghana: A focus on the Western Region. Heliyon, 4(2), e00534. https://doi.org/10.1016/j.heliyon.2018.e00534

Prasanth, S. S., Magesh, N. S., Jitheshlal, K. V., Chandrasekar, N., & Gangadhar, K. (2012). Evaluation of groundwater quality and its suitability for drinking and agricultural use in the coastal stretch of Alappuzha District, Kerala, India. Applied Water Science, 2(3), 165–175.

Ravikumar, P., Somashekar, R. K., & Angami, M. (2011). Hydrochemistry and evaluation of groundwater suitability for irrigation and drinking purposes in the Markandeya River basin, Belgaum District, Karnataka State, India. Environmental monitoring and assessment, 173(1), 459-487.

Richards, L. A. (1954). Diagnosis and improvement of saline and alkali soils (Handbook No. 60). U.S. Department of Agriculture.

Rivett, M. O., Buss, S. R., Morgan, P., Smith, J. W., & Bemment, C. D. (2008). Nitrate attenuation in groundwater: a review of biogeochemical controlling processes. Water research, 42(16), 4215-4232.

Ruiz-Pico, A., Cuenca, A. P., Serrano-Agila, R., Criollo, D. M., Leiva-Piedra, J., & Salazar-Campos, J. (2019). Hydrochemical characterization of groundwater in the Loja Basin (Ecuador). Applied Geochemistry, 104, 1–9. https://doi.org/10.1016/j.apgeochem.2019.02.012

Sappa, G., Ergul, S., Ferranti, F., 2014. Water quality assessment of carbonate aquifers in southern Latium region, Central Italy: a case study for irrigation and drinking purposes. Applied Water Science, 4(2), 115-128.

Shrestha, S., Kazama, F., (2007). Assessment of surface water quality using multivariate statistical techniques: A case study of the Fuji river basin, Japan.
Environmental Modelling and Software, 22(4), 464–475. https://doi.org/10.1016/j.envsoft.2006.02.001

Stallard, R. F., & Edmond, J. M. (1983). Geochemistry of the Amazon: 2. The influence of geology and weathering environment on the dissolved load. Journal of Geophysical Research: Oceans, 88(C14), 9671-9688.

Subba Rao, N., Subrahmanyam, A., Ravi Kumar, S., Srinivasulu, N., Babu Rao, G., Rao, P. S., & Reddy, G. V. (2012). Geochemistry and quality of groundwater of Gummanampadu sub-basin, Guntur District, Andhra Pradesh, India. Environmental Earth Sciences, 67(5), 1451-1471.

Sulaiman, M. A., Zafar, M. M., Prabhakar, R., Kumar, R., Sinha, R. K., & Kumari, A. (2024). A multivariate statistical approach to evaluate the hydro-geochemistry of groundwater quality in the middle Ganga river basin, Patna, India. Acta Geophysica, 72(3), 1913-1926.

Szabolcs, I., & Darab, K. (1964). Radio-active technique for examining the improving effect of $CaCO_3$ on alkali (Szik) soils. Acta Agronomica Hungarica, 13, 93–101.

WHO (1989). Health Guidelines for the Use of Wastewater in Agriculture and Aquaculture. Report of a WHO Scientific Group – Technical Report Series 778, WHO Geneva, 74 pp

WHO (2017). Guidelines for Drinking-water Quality: Fourth Edition Incorporating the First Addendum WHO, Geneva.

Wilcox, L. V. (1955). Classification and use of irrigation waters (USDA Circular No. 969, 19 pp.).

Williams, M., Fordyce, F., Paijitprapapon, A., & Charoenchaisri, P. (1996). Arsenic contamination in surface drainage and groundwater in part of the southeast Asian tin belt, Nakhon Si Thammarat Province, southern Thailand. Environmental Geology, 27(1), 16-33.

Yidana, S. M, Ophori, D and Banoeng-Yakubo, B. (2008). A multivariate statistical analysis of surface water chemistry – the Ankobra Basin, Ghana. Environ. Manag. 86, 80–87.